International Journal for Innovative Engineering and Management Research
A Peer Revieved Open Access International Journal
www.ijiemr.org

IJIEMR Transactions, online available on 10th Dec 2022. Link
:http://www.ijiemr.org/downloads.php?vol=Volume-11&issue=Issue 12

DOI: 10.48047/IJIEMR/V11/ISSUE 12/12

Title **MICRO-STRUCTURAL ANALYSIS OF SS304L AND SS308L IN HYBRID MANUFACTURING PROCESS WITH LAYER BY LAYER HEAT INPUTS VARIABILITY**

Volume 11, ISSUE 12, Pages: 75-81

Paper Authors
K.T.S.S. GANESH, V.V. D PRAVEEN KALEPU, A. SIRISHA BHADRAKALI

International Journal for Innovative Engineering and Management Research
A Peer Revieved Open Access International Journal
www.ijiemr.org

MICRO-STRUCTURAL ANALYSIS OF SS304L AND SS308L IN HYBRID MANUFACTURING PROCESS WITH LAYER BY LAYER HEAT INPUTS VARIABILITY

K.T.S.S. GANESH [1], V.V. D PRAVEEN KALEPU [2], A. SIRISHA BHADRAKALI [2]

[1] PG Scholar, Department of Mechanical Engineering, Aditya Engineering College(A), Surampalem

[2] Assistant Professor, Department of Mechanical Engineering, Aditya Engineering College(A), Surampalem

ABSTRACT:

In this study, a bimetallic additive manufactured surface is made by combining metal forming technology with wire arc additive manufacturing technology, a hybrid developed technique using diverse heat inputs. The SS304L hot-forged plate had SS308L placed on it using pulse mode WAAM technology. By variable heat input for layer deposition and the analysis for, microstructure of the specimen using SEM eds and XRD and concluded variable heat inputs enhances the microstructural properties.

KEY WORDS: WAAM, Metal Forming, Hybrid manufacturing, SS304L, SS308L, Metallurgical characteristics.

1. INTRODUCTION

[1]. The method of producing an object layer by layer is known as additive manufacturing. It is the reverse of subtractive manufacturing, which involves removing small amounts of a solid block of material at a time until the finished item is produced.

[2]. As a new the use of additive manufacturing in industry makes items by layering on materials, and as a result, may create custom parts with a previously unheard-of degree of freedom. During additive manufacturing, distinctive hierarchical microstructures are built for metallic materials, giving them a variety of fantastic features.

[3]. Due to the growing demand for efficient and environmentally friendly practises in the concrete construction sector along with cutting-edge technology enablers. The field of The field of in-situ additive manufacturing (AM) is now active in both academic research and commercialization.

[4]. In the current study, functionally graded material (FGM) with a seamless composition transition from 100 weight percent Inconel 625 (IN625) to 100 weight percent stainless steel 308 L was produced using dual wire arc additive manufacturing. With such a composition transition, the problem could be fully revealed because the place in the composition gradient route with the worst mechanical qualities could be identified plainly and simply. Cracks were discovered during manufacture close to the 20-weight percent position with IN625. By looking at the shape of the fracture and the location of the crack, they were classified as liquation fractures, which are hot cracks.

[5]. In this study, a functionally graded material (FGM) part was created using twin-wire and arc additive manufacturing by depositing a Cu-based alloy on top of a high strength low alloy (HSLA) steel (T-WAAM). Many industries are interested in copper and steel components because they can combine great mechanical qualities with strong thermal and electrical conductivity.

[6]. Researchers focused on the analysis of thermal behaviour in WAAM and worked on their determination.

[7]. Al-Cu-Sn alloy was employed as the starting material for this experiment and Using wire-arc additive manufacturing (WAAM), create deposits with various heat inputs. Investigations were done into how heat input affected the rheology and automated characteristics of Deposits of the alloy AlCuSn. metallography, energy dispersive spectroscopy (EDS), mechanical property testing, scanning electron microscopy, and transmission electron microscopy. The findings demonstrate that as the heat input was increased, the deposits' thickness and layer height grew.

[8]. Investigated were the fatigue strength and fatigue crack growth (FCG) behaviour created using the laser powder bed fusion (LB-PBF) method and 304L stainless steel (SS). Given that the alloy experiences a stress-induced martensitic transition that is temperature-dependent (SIMT),

International Journal for Innovative
Engineering and Management Research
A Peer Revieved Open Access International Journal
www.ijiemr.org

the effects were determined for construction orientation, microstructure, and temperature.

[9]. In this study, the standard of thin walls in construction made of 308L stainless steel was examined in relation to the gas-metal arc welding (GMAW) additive manufacturing deposition speed and temperature cycles. The findings show that the quality of the parts produced is in essence influenced by the deposition speed and thermal body clock. The surface waviness improves having a faster deposition rate.

[10]. By scanning using, the Scanning Electron Microscope, the materials surface mechanical properties can be examined in detail.

[11]. The widely used wire feed additive manufacturing technique known as wire arc additive manufacturing (WAAM) uses layer-by-layer material deposition to build components. Due to its high deposition rate, environmental friendliness, and cost-competitiveness, WAAM has emerged as a possible substitute for conventional machining. It is employed to create intricately formed pieces. Current, welding speed, shielding gas, and gas flow rate are the changeable parameters. 316 L stainless steel (WAAM plate) is fabricated in this study using a wire arc welding robot machine. Microwire cut EDM is used to remove the substrate and side edges, and a vertical milling machine is used to complete the surface. Tensile strength, hardness, and X-ray diffractive properties are compared to stainless steel standard 316 L. Utilizing COMSOL Multiphysics, 316L stainless steel is modelled and analyzed.

2. MATERIALS AND METHODOLOGY

2.1 MATERIALS:

STAINLESS STEEL 304 L (BASE PLATE):

The minimum nickel and chromium content of stainless-steel alloy 304L, a T-300 class austenitic, is 8% and 18%, respectively. The highest permitted carbon content for type 304L is 0.030. Cookware and kitchen equipment are typically made with the standard "18/8 stainless." Alloy 304L is the most widely used and versatile stainless-steel alloy. Alloy 304L is ideal for a number of home and commercial applications because to its excellent formability, high ease of production, and great corrosion resistance. The most weldable high-alloy steels are austenitic sinless steels, which can be joined using any fusion or resistance welding method.

STAINLESS STEEL 308 L:

Grade 308L stainless steel is a low carbon variant of grade 308. Utilizing a submerged arc, it is specifically designed to weld grade 304 stainless steel. It can also be used to weld stabilised grades 321 and 347 in non-corrosive situations.

The mechanical and physical characteristics of SS304L and SS308L are shown in Tables 1 and 2, respectively.

GRADE	TENSILE STRENGTH KSI (MPA)	HARD NESS (BRINELL) MAXI	HARDNESS (ROCKWELL B) MAXI
304L	70 (485)	201	92
308L	88 (593)	170	87

Table 1: **Mechanical Properties**

International Journal for Innovative Engineering and Management Research
A Peer Revieved Open Access International Journal
www.ijiemr.org

GRADE	DENSITY g/cm3	THERMAL CONDUCTIVITY (W/m-K)	ELECTRICAL RESISTIVITY (in x 10-6)	COEFFICIENT OF THERMAL EXPANSION (in/in) / °F x 10-6	SPECIFIC HEAT (BTU/lb/ °F)	MELTING RANGE R (°F)
304L	7.93	16.2 at 100°C 21.5 at 500°C	28.4 at 68°F	9.5 at 32 – 212°F	0.1200 at 68°F to 212°F	2500.1to 2590.1
308L	7.84	15 at 100°C 20.2 at 500°C	26.3 at 68°F	9.7 at 32 – 212°F	0.11 at 68°F to 212°F	1380.1 to 2510.1

Table 2: **Physical Properties**

2.2 METHODOLOGY

In this project, a hybrid production process combining forging and wire arc additive manufacturing was used. SS308L MIG wire with a 1.2mm diameter was used for deposition utilizing GMAW-WAAM on a forging stainless steel 304L plate. In order to achieve better outcomes during deposition, pulse mode in GMAW-WAAM was applied [12]. In order to evaluate the temperature effects on mechanical qualities in the Wire and Arc Additive Manufacturing method, the heat input for deposition was changed while depositing. Researchers established that the WAAM deposition technique performs better using a two-tier input system [13]. In this experiment, layer-by-layer deposition on a forged plate was done using a two-tier heat input method. while depositing on a forged plate.

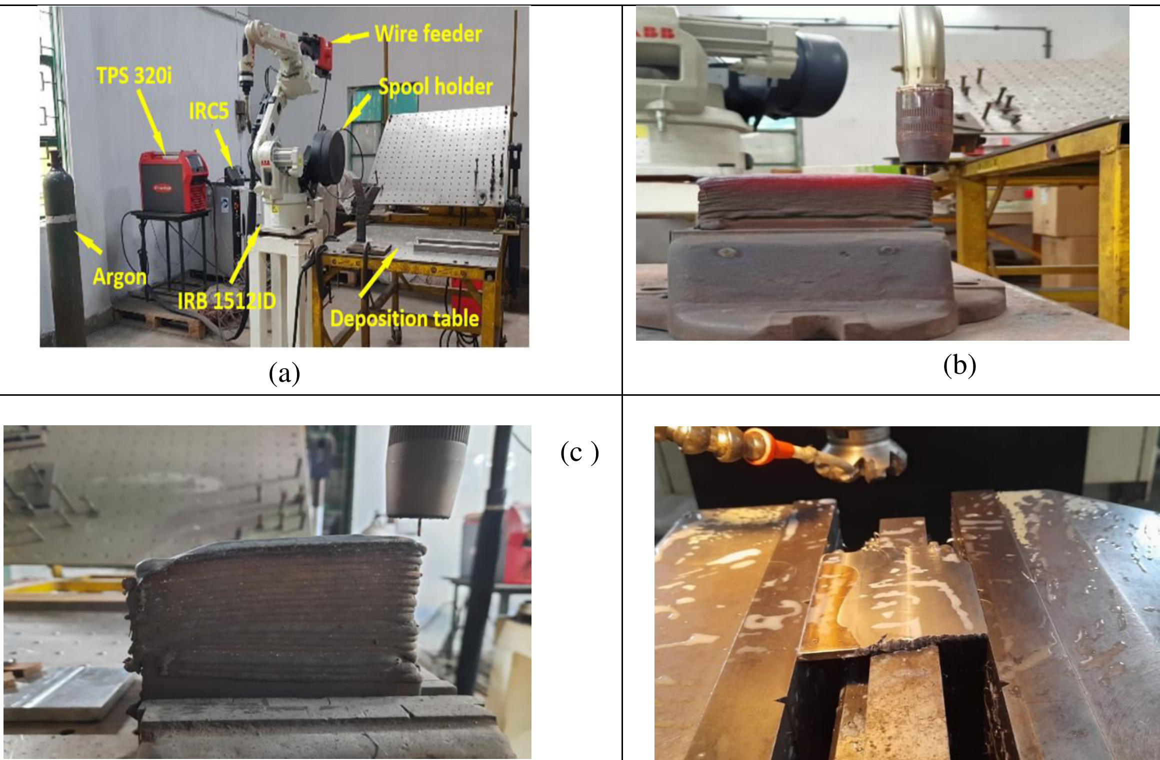

(a) (b) (c) (d)

Fig 1: (a) Experimental set up (b) Deposition on forged plate (c) Final specimen (d) Post processing of plate

International Journal for Innovative Engineering and Management Research
A Peer Revieved Open Access International Journal
www.ijiemr.org

The experiment makes use of the parameters listed in table 3 below. These characteristics change from one layer to the next. The first layer was started with a high heat input and given a 10-second cooling period before deposition of the second layer began with a low heat input. In a similar manner, each layer was laid down. On the forged plate, a total of 36 layers were deposited to achieve the desired height. Table 4 provided a detailed breakdown of the heat input each layer.

Table 3: Process parameters in the Experimentation

LAYER	I_m (Amp)	V_m (Volt)	f (Hz)	T S (mm/sec)	H I (J/mm)	I_p (Amp)	I_b (Amp)	t_p (sec)	t_b (sec)
1	147	20.3	0.5	6	422.75	250	78.31	0.81	1.23
2	119	11	0.4	5	222.139	204	64.1	0.71	1.01

LAYER NO	VOLTAGE	CURRENT	TS (mm/sec)	HI (J/mm)
1	147	20.3	6	422.75
2	119	11	5	222.12
3	119	11	5	222.12
4	147	20.3	6	422.75
5	119	11	5	222.12

Table 4: Layer wise heat input in the Experimentation

2.2.1 SCANING ELECTRON MICROSCOPE (SEM):

Microstructural analysis was done at three different zones that is
(a) Base zone
(b) Interface zone
(c) Deposited zone
I used the Scanning Electron Microscope (SEM) test and the X-Ray Diffraction (XRD) test to observe the microstructure in these three zones.
Scanning Electron Microscope analysis is not alone cannot give the better results. so along with EDS was done .and XRD also performed at the three zones.
Following various the different magnification was taken at three different zones.

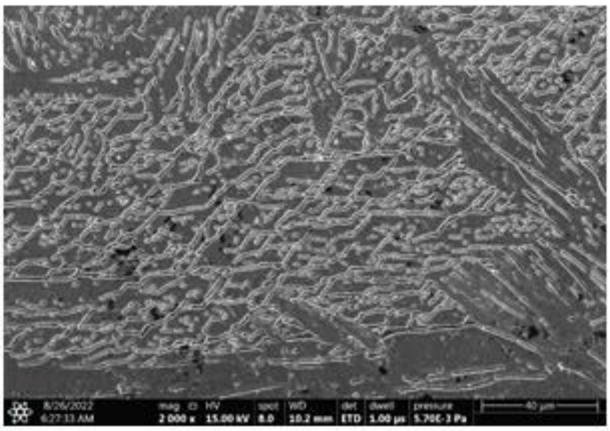

International Journal for Innovative Engineering and Management Research
A Peer Revieved Open Access International Journal
www.ijiemr.org

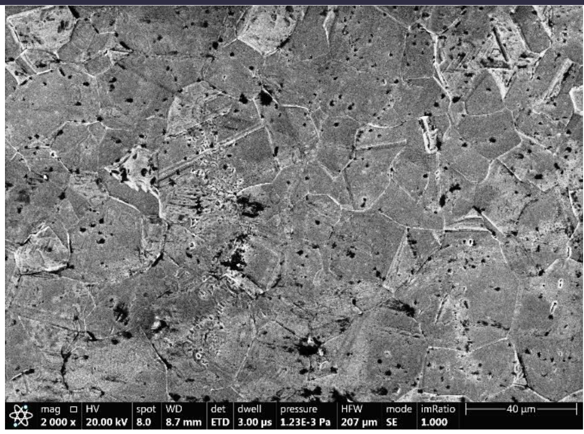

Fig 2: (a) base zone (b) interface zone

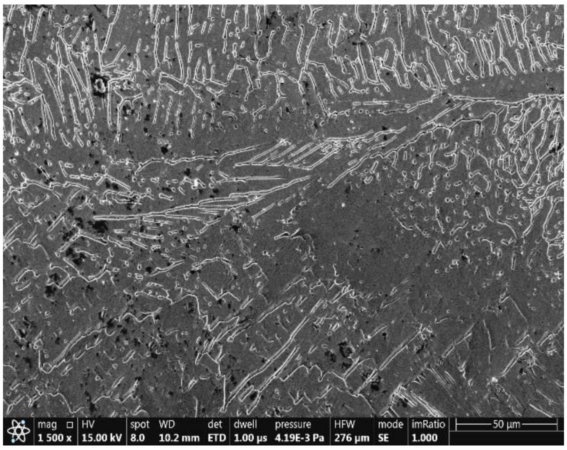

(c) deposited zone

Here we examined the micro-structure of the sample using Scanning electron microscope method and found that

In the scanning electron microscope and Electron Diffraction test, the Ferrous (Fe) weight in the base zone was found to be 67.28%, Interface zone Ferrous (Fe) weight is 70.16% and Deposited zone Ferrous (Fe) weight is 69.24%. Chromium (Cr) weight in the Base zone 18.32%, Interface zone Chromium (Cr) weight is 18.52 % and Deposited zone of Chromium (Cr) weight 18.91%. In this experiment Nickel (Ni) weight in Base zone is 7.34% & Interface zone Nickel (Ni) weight is 6.69% and deposited zone Nickel (Ni) weight is 6.91. In this test carbon (C) Base zone weight is 2.83% & Interface zone carbon (C) weight is 1.86% and Deposited zone weight is carbon(C) 2.58%. Manganese (Mn) Based zone weight is 2.71%& Manganese (Mn) Interface zone weight is 2.36% and Deposited zone of Manganese (Mn) weight is 1.89%. in this experiment Silicon (Si) Base zone weight is 0.33& Interface zone of Silicon (Si) weight is 0.42% and Deposited zone of Silicon (Si) weight is 0.47% and finally oxygen base zone weight is 0.65%. The ferrous weight was high in the scanning electron microscope test. Chromium is next in weight on this experiment. In this experiment, the least weight percentage contains is Si and oxygen.

2.2.2 X-RAY DIFFRACTION:

A potent, unobtrusive method for characterizing crystalline materials is x-ray diffraction. that gives specific information about the physical attributes, chemical makeup, and crystallographic structure of materials. The crystallite sizes of the specimen at the various three zones were observed using X-ray diffraction. Based on the experimentally forged peak values, we calculated the crystallite sizes using the Scherrer Equation as described below and discovered that the crystallite sizes have been improved. By using Scherrer Formula and calculate the crystallite size. It is the size of a crystal fragment that coherently diffracts light. A beam of electrons strikes a revolving target and emits the resulting x rays. Targets like the cu are kept cool by having a stream of cold water available and

International Journal for Innovative Engineering and Management Research
A Peer Revieved Open Access International Journal
www.ijiemr.org

whirling at a pace of 6000 rpm to prevent heating. this produces an x-ray continuum. But we're looking for a specific k alpha wavelength. Before, some filters were employed (thin ni foil in case of cu). Nowadays, monochromators like quartz crystal are employed. Finally, the sample is struck by these x rays, which are detected by a detector's photomultiplier tube. In conclusion, it may be said that a peak's overall strength results from the superposition of all helpful and harmful contributions, which is undoubtedly influenced by the atomic positions.

D p = (0.94 X λ) / (β X Cos θ) Where, D p = Average Crystallite size, β = Line broadening in radians, θ = Bragg angle, λ = X-Ray wavelength .X-ray diffraction forged zone crystallite average size result is 51nm.Base zone crystallite average size result is 51.0066nm, Interface zone crystallite average size result is 49.6375nm and Deposited zone crystallite average size results is 45.89nm.

In this Graph black colour line denoted by Forged zone, red colour denotes by Base zone of the material, blue colour denoted by Interface zone of the material and purple colour denoted by deposited zone. We have taken 2 theta angles on x in the graph & Intensity (a. u) on Y in the graph.

In this graph lattice structure of 111, 200, 220 is miller index and reciprocal values considered. When observed the graph (Fig:2) the crystallite XRD size is Big .

3.RESULT:

By using the Scanning Electron Microscope (SEM) the dendrite structure of the specimen at the three different zones were observed and found that the micro-structural properties have been enhanced due to variable heat inputs. In the test using a scanning electron microscope, the ferrous weight was high. On this experiment, chromium is weighed next. Si and oxygen make up the least amount of the total weight in this experiment.

By using X-ray Diffraction, the crystallite size of the specimen at the different three zones were observed and based on the experimental forged peak values calculated the crystallite sizes by using Scherrer Equation as mentioned below and found that the crystallite sizes have been enhanced.

Scherrer Formula:

$$D_p = (0.94 \times \lambda) / (\beta \times \cos\theta)$$

Where, D p = Average Crystallite size, β = Line broadening in radians, θ = Bragg angle, λ = X-Ray wavelength. The crystallite sizes of forged plate are 51nm. crystallite XRD size is Big.

4.CONCLUSION:

Forging hybrid products with wire arc additive Layer by layer manufacturing using variable heat inputs was successfully implemented in the SS300 Series. This experiment led to the following conclusion:

- Even though the heat input decreases during the deposition of subsequent layers, the corresponding heat input is still sufficient to melt the previous layer (or at least one previously deposited layer). As a result, it produces strong metallurgical bonding between the layers, fulfilling the GMAW-WAAM process's requirement for inter-layer bonding.
- Variable heat input shows that there is enhancement in crystallite size which leads to better metallurgical characteristics.
- Also, more amount of Ferrous and Chromium content can led to enhancement in the micro structural and mechanical properties of specimen.

REFERNCES:

[1]. Ainapurapu, Sirisha Bhadrakali, et al. "Microstructure and Mechanical Properties of the Bimetallic Wire Arc Additively Manufactured Structure (BAMS) of SS304L and SS308L Fabricated by Hybrid Manufacturing Process." *Transactions of the Indian Institute of Metals*, 10 Aug. 2022, 10.1007/s12666-022-02695-2. Accessed 9 Sept. 2022.

[2]. Dörfler, Kathrin, et al. "Additive Manufacturing Using Mobile Robots: Opportunities and Challenges for Building Construction." *Cement and Concrete Research*, vol. 158, Aug. 2022, p. 106772, 10.1016/j.cemconres.2022.106772. Accessed 19 June 2022.

[3]. Kumar, Punit, et al. "Role of Metastable Austenite in the Fatigue Resistance of 304L Stainless Steel Produced by Laser-Based Powder Bed Fusion." *Materials Science and Engineering: A*, vol. 837,

Mar. 2022, p. 142744, 10.1016/j.msea.2022.142744. Accessed 29 Nov. 2022.

[4]. Le, Van Thao, et al. "Influences of the Process Parameter and Thermal Cycles on the Quality of 308L Stainless Steel Walls Produced by Additive Manufacturing Utilizing an Arc Welding Source." *Welding in the World*, vol. 66, no. 8, 17 June 2022, pp. 1565–1580, 10.1007/s40194- 022-01330-4. Accessed 29 Nov. 2022.

[5]. Li, Tianxu, et al. "Hot Cracking during the Fabrication of Inconel 625/Stainless Steel 308 L Functionally Graded Material by Dual-Wire Arc Additive Manufacturing." *Journal of Manufacturing Processes*, vol. 82, Oct. 2022, pp. 461–473, 10.1016/j.jmapro.2022.08.018. Accessed 29 Nov. 2022.

[6]. Madhavadas, Vaishnav, et al. "A Review on Metal Additive Manufacturing for Intricately Shaped Aerospace Components." *CIRP Journal of Manufacturing Science and Technology*, vol. 39, 1 Nov. 2022, pp. 18–36, www.sciencedirect.com/science/article/abs/pii/S1755581722001304?casa_token=C7ioFCpt7O8AAAAA:Otz1nANwd8rBWRL32kV8VwTW_ToKYLmY4jqxiktQfcJEvhUvQxyXOP_DMZpqvKdYYjnZHwWX0nM, 10.1016/j.cirpj.2022.07.005. Accessed 14 Oct. 2022.

[7]. Rodrigues, Tiago A., et al. "Steel-Copper Functionally Graded Material Produced by Twin-Wire and Arc Additive Manufacturing (T-WAAM)." *Materials & Design*, vol. 213, 1 Jan. 2022, p. 110270, www.sciencedirect.com/science/article/pii/S026412752100825X, 10.1016/j.matdes.2021.110270. Accessed 5 July 2022.

[8]. Srivastava, Shekhar, et al. "A Multi-Tier Layer-Wise Thermal Management Study for Long-Scale Wire-Arc Additive Manufacturing." *Journal of Materials Processing Technology*, vol. 306, Aug. 2022, p. 117651, 10.1016/j.jmatprotec.2022.117651. Accessed 29 Nov. 2022.

[9]. Tankova, Trayana, et al. "Characterization of Robotized CMT-WAAM Carbon Steel." *Journal of Constructional Steel Research*, vol. 199, Dec. 2022, p. 107624, 10.1016/j.jcsr.2022.107624. Accessed 1 Dec. 2022.

[10]. Xu, Yi-Peng, et al. "Risk-Averse Multi-Objective Optimization of Multi-Energy Microgrids Integrated with Power-To-Hydrogen Technology, Electric Vehicles and Data Center under a Hybrid Robust-Stochastic Technique." *Sustainable Cities and Society*, vol. 79, Apr. 2022, p. 103699, 10.1016/j.scs.2022.103699. Accessed 10 Nov. 2022.

[11]. Yildiz, Ahmet Suat, et al. "Thermal Behavior Determination for Wire Arc Additive Manufacturing Process." *Procedia Manufacturing*, vol. 54, 2021, pp. 233–237, 10.1016/j.promfg.2021.07.036. Accessed 11 Jan. 2022.

[12]. Vinoth, V., S. Sathiyamurthy, J. Prabhakaran, Harsh Vardhan, and S. Sundaravignesh. "Tensile, Hardness, XRD and Surface Vonmises Stress of 316 L Stainless Steel Built by Wire Arc Additive Manufacturing (WAAM)." *Journal of Manufacturing Engineering* 17, no. 3 (2022): 098-103.

[13]. Wang, Shuai, et al. "The Influence of Heat Input on the Microstructure and Properties of Wire-Arc-Additive-Manufactured Al-Cu-Sn Alloy Deposits." *Metals*, vol. 10, no. 1, 2 Jan. 2020, p. 79, 10.3390/met10010079. Accessed 12 Feb. 2020.